

---

## Properties of Cryoliquids

In this chapter, I shall discuss properties of cryoliquids important for the design and performance of low-temperature experiments. Of course, cryoliquids are very important for low-temperature physics because they are the simplest means of achieving low temperatures. In particular, the properties of liquid helium are essential because all refrigeration methods to  $T < 10\text{ K}$  use liquid helium as a final or intermediate refrigeration stage. I shall not discuss the technology of liquefaction [2.1, 2.2]. For liquifaction the gas has to be isothermally compressed and then expanded to let it perform “external” work (for example, in an expansion engine), or perhaps using the well-known Joule–Thomson effect, which means letting the gas expand and perform “internal” work against the mutual attraction of its atoms or molecules. This latter effect leads to cooling if the starting temperature is below the inversion temperature  $T_i$ , which is  $6.75 T_c$ ,  $T_c$  being the critical temperature for a van der Waals gas. Various properties of cryoliquids are summarized in Table 2.1 and are compared there to the relevant properties of water. Of particular importance for refrigeration are the boiling point  $T_b$  (defining the accessible temperature range), the latent heat of evaporation  $L$  (defining the cooling power) and – last but by no means least important – the price (defining the availability).

### 2.1 Liquid Air, Liquid Oxygen, Liquid Nitrogen

Today liquid oxygen is not in common use as a refrigerant because it is extremely reactive. An explosive oxidation reaction can occur if the oxygen comes into contact with organic liquids, like oil used in pumps, or with solid matter having a large surface area, like metal powder. The boiling temperature of oxygen lies above the boiling temperature of nitrogen. Therefore, if one keeps liquid air in a container, the nitrogen evaporates first, resulting in an enrichment of liquid oxygen, and thus eventually leading to this dangerous liquid again. For these reasons, today air is liquefied and separated into oxygen and nitrogen in large liquefaction and separation plants. Liquid

**Table 2.1.** Properties of some liquids ( $T_b$  is the boiling point at  $P = 1$  bar,  $T_m$  the melting point at  $P = 1$  bar,  $T_{tr}(P_{tr})$  the triple-point temperature (pressure),  $T_c(P_c)$  the critical temperature (pressure), and  $L$  the latent heat of evaporation at  $T_b$ ). The data have mostly been taken from [2.3–2.5, 2.17]

subst.	$T_b$ (K)	$T_m$ (K)	$T_{tr}$ (K)	$P_{tr}$ (bar)	$T_c$ (K)	$P_c$ (bar)	lat. heat, $L$ (kJl <sup>-1</sup> )	vol% in air
H <sub>2</sub> O	373.15	273.15	273.16	0.06*	647.3	220	2,252	–
Xe	165.1	161.3	161.4	0.82	289.8	58.9	303	$0.1 \times 10^{-4}$
Kr	119.9	115.8	114.9	0.73	209.4	54.9	279	$1.1 \times 10^{-4}$
O <sub>2</sub>	90.1	54.4	54.36	0.015	154.6	50.4	243	20.9
Ar	87.2	83.8	83.81	0.69	150.7	48.6	224	0.93
N <sub>2</sub>	77.2	63.3	63.15	0.13	126.2	34.0	161	78.1
Ne	27.1	24.5	24.56	0.43	44.5	26.8	103	$18 \times 10^{-4}$
<i>n</i> -D <sub>2</sub>	23.7	18.7	18.69	0.17	38.3	16.6	50	–
<i>n</i> -H <sub>2</sub>	20.3	14.0	13.95	0.07	33.2	13.2	31.8	$0.5 \times 10^{-4}$
<sup>4</sup> He	4.21	–	–	–	5.20	2.28	2.56	$5.2 \times 10^{-4}$
<sup>3</sup> He	3.19	–	–	–	3.32	1.15	0.48	–

\* The exact value is  $P_{tr} = 61.1657$  mbar

nitrogen (LN<sub>2</sub>) is then sold as a refrigerant at roughly  $0.25 \text{ € l}^{-1}$  when delivered in large quantities. Very few research organizations still use their own liquefaction plant as was common until the 1960s.

Evaporating nitrogen can cause suffocation if it displaces much of the usual 20% oxygen in an enclosed volume. Therefore, rooms in which evaporating liquid nitrogen is kept have to be fitted with an appropriate ventilation system.

## 2.2 Liquid Hydrogen

In liquid hydrogen the pair of atoms forming an H<sub>2</sub> molecule are bound by a strong covalent force. The interactions between H<sub>2</sub> molecules, which lead to the liquid and solid states, are the weak van der Waals forces. These weak dipolar forces, as well as the large zero-point motion of the light H<sub>2</sub>, result in rather low boiling and melting points (Table 2.1). Because of the large difference in strength between chemical bonds and dipolar forces, liquid and solid H<sub>2</sub> are true molecular fluids and crystals in which the molecules retain many of the properties of free H<sub>2</sub> [2.6, 2.7].

The dangerous feature of hydrogen is its exothermic reaction with oxygen to form water. Therefore, liquid hydrogen should be used in a closed system. However, sometimes the danger associated with hydrogen is over-estimated because the reaction needs a concentration of more than 4% in air in order to occur.

Whereas at one time liquid hydrogen was frequently used as a refrigerant (and its use may become more common in hydrogen energy technologies in the future), it is not often used in laboratories these days because the temperature

range between the boiling point of nitrogen (77 K) and the boiling point of helium (4.2 K) is now accessible by means of closed-cycle refrigerators (Sect. 5.3), helium evaporation cryostats (Sect. 5.2.3) or by performing the experiment in helium gas above a liquid-helium bath.

In spite of the minor importance of hydrogen as a refrigerant I shall discuss one of its properties which is important in various low-temperature experiments and which demonstrates some rather important atomic and statistical physics: the *ortho-para* conversion of  $\text{H}_2$  [2.6–2.12].

The proton H has a nuclear spin  $I = 1/2$ . In a  $\text{H}_2$  molecule the two nuclear spins can couple to a total spin  $I = 0$  or  $I = 1$ , depending on their relative orientation. Thus, the  $\text{H}_2$  molecule can have a symmetric nuclear state ( $I = 1$ ), so-called *ortho- $\text{H}_2$* . This system has a degeneracy of  $2I + 1 = 3$ , which means that it can exist in three different spin orientational states, namely  $m = -1, 0, +1$ . For the other total-spin situation ( $I = 0$ ) we have an anti-symmetric state, so-called *para- $\text{H}_2$* , with the degeneracy  $2I + 1 = 1$ , which means that this system can only exist in one spin state,  $m = 0$ .

In addition, the non-spherical  $\text{H}_2$  molecule can rotate and we have the  $\text{H}_2$  rotator with the rotational quantum numbers  $J = 0, 1, 2, 3, \dots$ . Because of the weak interaction between  $\text{H}_2$  molecules, the behavior of the rotator is free and  $J$  remains a good quantum number. The various rotational states are separated by rotational energies:

$$E_R = \frac{\hbar^2}{2\theta} J(J + 1), \quad (2.1)$$

where  $\theta = 4.59 \times 10^{-48} \text{ kg m}^2$  is the moment of inertia of the  $\text{H}_2$  rotator.

Protons are Fermi particles (fermions). As a result, the total wave function of the  $\text{H}_2$  molecule has to be anti-symmetric under an exchange of particles. In other words, it has to change its sign if the two nuclei are exchanged. The total wave function is a product of the spin wave function and the spatial wave function (electronic and vibronic excitations are negligible at  $T < 1,000 \text{ K}$ ). To get an anti-symmetric total wave function either the spin or the rotator wave function has to be anti-symmetric and the other one has to be symmetric. This results in two possibilities for the hydrogen molecule, which are summarized in Table 2.2.

The energy states of *para-* and *ortho-*hydrogen are depicted in Fig. 2.1. The total degeneracy of each rotational state is given by  $d = (2J + 1)(2I + 1)$ .

**Table 2.2.** Properties of *ortho-* and *para-*hydrogen

Molecule	Nuclear spin, $I$	Symmetry	Deg.	Rotator quantum number, $J$	Symmetry	Deg.
<i>Ortho-<math>\text{H}_2</math></i>	1	Symmetric	3	1, 3, ...	Anti-symmetric	3, 7, ...
<i>Para-<math>\text{H}_2</math></i>	0	Anti-symmetric	1	0, 2, ...	Symmetric	1, 5, ...

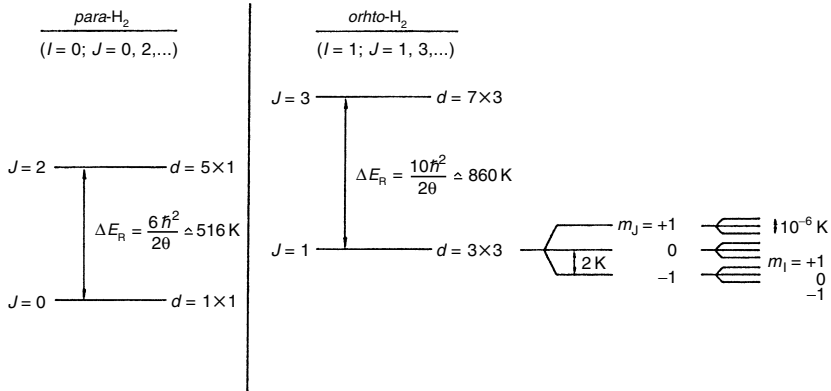


**Fig. 2.1.** Rotational energy states of *para*- and *ortho*-H<sub>2</sub>. The degeneracy of the rotational states of *ortho*-H<sub>2</sub> is lifted by an electric quadrupole interaction between the H<sub>2</sub> molecules which is of order 2 K. A nuclear magnetic dipole interaction of order 10<sup>-6</sup> K lifts the nuclear magnetic degeneracy of the *m<sub>J</sub>* states

Because of the rather large energies  $\Delta E_R$  separating the various rotator states, only the lowest rotational energy states are significantly populated at room temperature or lower temperatures. Owing to this fact and because of the different rotational degeneracies as well as of the threefold nuclear degeneracy of *ortho*-H<sub>2</sub>, we have 25% *para*-hydrogen and 75% *ortho*-hydrogen in thermal equilibrium at room temperature. Because *para*-H<sub>2</sub> ( $J = 0$ ) has lower energy than *ortho*-H<sub>2</sub> ( $J = 1$ ) (the difference is 172 K if expressed in terms of temperature), a conversion from *ortho*- to *para*-hydrogen occurs if we cool hydrogen to low temperatures. Their ratio is given by

$$\frac{N_{ortho}}{N_{para}} = \frac{3 \sum_{J=1,3,\dots} (2J + 1) e^{-\hbar^2 J(J+1)/(2\theta \cdot k_B T)}}{\sum_{J=0,2,\dots} (2J + 1) e^{-\hbar^2 J(J+1)/(2\theta \cdot k_B T)}} \quad (2.2)$$

This ratio is illustrated in Fig. 2.2. At 77 K the equilibrium ratio is 1:1, but at 20 K we should have 99.8% *para*-H<sub>2</sub> in thermal equilibrium.

We have to take into account two important aspects of this conversion. First of all, it is an exothermic reaction giving rise to the rather large heat release of  $U = 1.06$  (1.42) kJ mol<sup>-1</sup>H<sub>2</sub> for a starting *ortho* concentration of 75% (100%). Secondly, the conversion between different rotational states is connected with a change of the nuclear spin orientation. For this change of the nuclear quantum state, we need an interaction of the nuclear magnetic moments with each other or with changing magnetic fields in their surroundings. Because of the smallness of the nuclear moments this nuclear dipolar interaction is rather weak. It can only occur in the collision of two H<sub>2</sub> molecules if there is no other magnetic partner available. We then have an autocatalytic reaction and, due to its weakness, the conversion is slow with an *ortho*-to-*para*

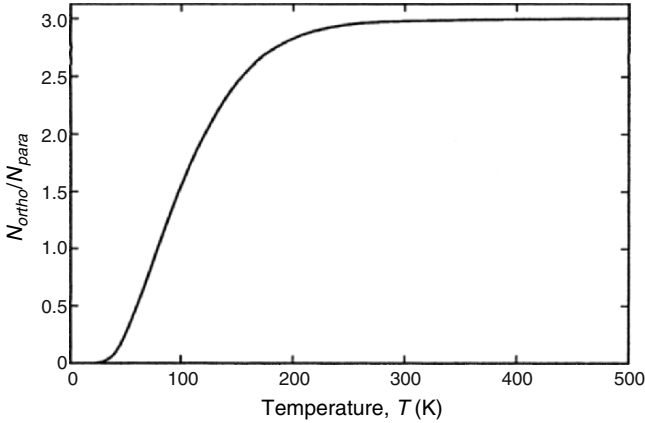


**Fig. 2.2.** Ratio of *ortho*-to-*para* hydrogen as a function of temperature

rate constant of  $k = 1.8\%$  per hour for solid  $H_2$  at melting pressure [2.10,2.13], leading to interesting time effects.

Let us calculate the heat release due to this conversion. The change of the concentration  $x$  of the *ortho* molecules with time  $t$  for this autocatalytic reaction is given by

$$\frac{dx}{dt} = -kx^2, \quad (2.3)$$

resulting in

$$x(t) = \frac{x_0}{1 + x_0kt}, \quad (2.4)$$

where  $x_0$  is the starting *ortho* concentration, which is 0.75 for  $T = 300$  K. This gives rise to the molar heat release

$$\dot{Q} = -U \frac{dx}{dt} = U \frac{kx_0^2}{(1 + x_0kt)^2}. \quad (2.5)$$

There are two situations in which this heat release can give rise to problems in experiments at low or ultralow temperatures. First, we have to keep in mind that the heat release due to *ortho-para* conversion is quite large. Therefore, if one has a liquid consisting mainly of *ortho*-hydrogen it will evaporate due to the *ortho-para* conversion even without any extra external heat being introduced. As a result, one has first to convert the *ortho*- $H_2$  to *para*- $H_2$  before the liquid can be used as a refrigerant. The conversion is strongly accelerated if the  $H_2$  is brought into contact with a catalyst containing electronic magnetic moments, e.g., ferric hydroxide, iron or chromic oxide [2.2,2.11], or oxygen [2.12], because then the small *nuclear* magnetic moment of one of the two interacting O- $H_2$  is replaced by the much larger *electronic* magnetic moment of the catalyst. The conversion equation is then changed to

$$dx/dt = -kx^2 - k_1xx_1, \quad (2.6)$$

where  $k_1$  is the conversion rate constant for the catalyzed reaction and  $x_1$  is the concentration of the paramagnetic impurity. Because of the temperature dependence of the diffusion time of the *o*-H<sub>2</sub> molecule to the paramagnetic impurity,  $k_1$  is temperature dependent at  $T < 10$  K. At higher temperatures,  $k_1 = 1.15\%$  per second (!) for solid H<sub>2</sub> containing  $x_1 = 100$  ppm O<sub>2</sub> only, as an example [2.12]. In *pure* liquid and gaseous H<sub>2</sub>, the *ortho*- to *para*-conversion rate constant is (3 to 22)  $10^{-3}$  per hour (!) for H<sub>2</sub> densities between 0.02 and 0.1 g cm<sup>-3</sup> and at temperatures from 16 to 120 K [2.13].

The second problem became apparent with the advent of ultralow-temperature physics, where the refrigeration power of refrigerators can become rather small (in the microwatt range for low millikelvin temperatures and in the nanowatt range for microkelvin temperatures; see Chaps. 7–10). Many metals, such as palladium and niobium, can dissolve hydrogen in atomic form in their lattice. However, many others such as Cu, Ag, Au, Pt and Rh, cannot dissolve hydrogen in a noticeable quantity in their lattice. If these metals contain traces of hydrogen, hydrogen molecules collect in small gas bubbles with a typical diameter of some 0.1  $\mu\text{m}$  [2.14]. In practice, many of these metals contain hydrogen at a typical concentration of 10–100 ppm due to their electrolytic production or from a purification process. The hydrogen pressure in these small bubbles is so high that the hydrogen becomes liquid or solid if the metal is cooled to low temperatures. This then results again in a conversion from *ortho*- to *para*-hydrogen in the small bubbles, and therefore gives rise to

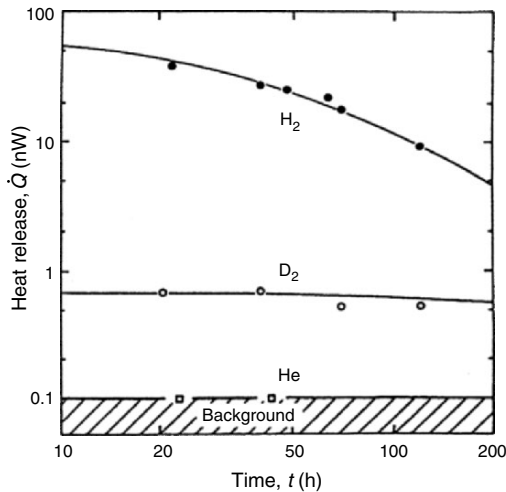


**Fig. 2.3.** Heat release at  $T \leq 0.1$  K from 19 g Cu samples charged at 930°C in 3.05 bar of the indicated gases as a function of time after cooling to  $T \leq 4$  K. The upper *curve* represents (2.5) for 23  $\mu\text{mol}$  H<sub>2</sub> (76 ppm H<sub>2</sub>/Cu). The curve through the D<sub>2</sub> data is the corresponding equation for deuterium [2.9] for 25  $\mu\text{mol}$  D<sub>2</sub> (83 ppm D<sub>2</sub>/Cu). The Cu sample heated in an He atmosphere did not give a heat release above the indicate background value of the calorimeter [2.15]

heat release in these metals (Fig. 2.3) [2.15, 2.16]. The heat release is small, typically of the order of  $1 \text{ nW g}^{-1}$ , but it can be very detrimental if such a metal is used in an apparatus designed for ultralow-temperature physics experiments, such as a nuclear refrigerator for the microkelvin-temperature range (Sect. 10.5.3).

In addition to its importance for low- and ultralow-temperature physics and its nice demonstration of atomic and statistical physics, the *ortho-para* conversion also demonstrates in a rather impressive way how very little energy, in this case the nuclear magnetic interaction energy (which is of the order of microkelvins if expressed in temperatures), due to the existence of nuclear spins and in combination with the Pauli principle, can result in rather dramatic effects involving much higher energies, in this case the rotational energy of the order of 100 K.

## 2.3 Liquid Helium

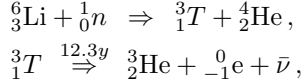
### 2.3.1 Some Properties of the Helium Isotopes

In 1868, the two scientists J. Janssen and N. Lockyer detected new spectral lines in the optical spectrum of the sun. First it was suggested that these lines might belong to an *isotope* of hydrogen or to sodium, but very soon it became evident that the spectral lines belonged to a new *element*, later called “helium”. In 1895 the British scientist W. Ramsey detected these lines on earth, in a gas escaping from the mineral cleveite. Two of the most eminent physicists of that time, J. Dewar in London and H. Kamerlingh Onnes in Leiden, began a race to liquefy this newly discovered element of the periodic table. H. Kamerlingh Onnes won this race, liquefying helium at a temperature of 4.2 K in 1908. The first commercial helium liquefier built by S.C. Collins in 1947 had a profound impact on the spread of low-temperature experiments because liquid helium is the most important substance for low-temperature physics. All refrigeration methods for temperatures below about 10 K either use liquid helium exclusively or, if they go to very low temperatures, use liquid helium in the pre-cooling stages. At first liquid helium was employed only as a tool, but research in the following decades made it very obvious that liquid helium is a most exotic and interesting liquid exhibiting many unique properties.

Whereas in the first years of helium research the  $^4\text{He}$  gas was obtained from minerals, today helium is obtained exclusively from helium-rich natural-gas sources. In both cases it is a product of radioactive alpha decay. The gas sources, particularly in the USA, North Africa, Poland, the Netherlands and the former USSR, can contain up to about 10% helium.

The common stable helium isotope is  $^4\text{He}$ . Its nucleus contains two protons and two neutrons, each with anti-parallel nuclear spin orientation. Therefore, the total nuclear spin of  $^4\text{He}$ ,  $I = 0$ ; it is a Bose particle (boson). The rare

helium isotope  ${}^3\text{He}$  constitutes a fraction  $(1-2) \times 10^{-7}$  of helium gas from natural gas sources and about  $1.3 \times 10^{-6}$  of the helium gas in the atmosphere. Obtaining  ${}^3\text{He}$  in a reasonable amount from these two sources by separating it from  ${}^4\text{He}$  is very costly. The  ${}^3\text{He}$  in use today for low-temperature physics experiments is a byproduct of tritium manufacture in a nuclear reactor:



where  $\bar{\nu}$  is the electron anti-neutrino. The helium isotopes are separated from tritium by diffusion processes. Due to this method of production,  ${}^3\text{He}$  has only been available in necessary quantities since the late 1950s, and it is expensive (about  $200 \text{€ l}^{-1}$  of gas at standard temperature and pressure). The  ${}^3\text{He}$  nucleus again contains two protons, but only one neutron. Therefore, its total nuclear spin  $I = 1/2$ , and  ${}^3\text{He}$  is a fermion. The different statistics for the boson  ${}^4\text{He}$  and for the fermion  ${}^3\text{He}$  cause substantial differences in their low-temperature behavior, some of which will be discussed in the following pages. Details can be found in [2.17–2.24].

Besides the stable isotopes  ${}^3\text{He}$  and  ${}^4\text{He}$ , there exist two unstable helium isotopes with relatively long lifetimes:  ${}^6\text{He}$  ( $\tau_{1/2} = 0.82 \text{ s}$ ), and  ${}^8\text{He}$  ( $\tau_{1/2} = 0.12 \text{ s}$ ); they have not yet been liquified.

In Table 2.3 some important properties of the two stable helium isotopes are summarized and their pressure–temperature phase diagrams are shown in Fig. 2.4. The table and the figure demonstrate some of the remarkable properties of these so-called quantum substances. First, there are their rather low boiling points and critical temperatures. Then, unlike all other liquids these two isotopes do not become solid under their own vapour pressure even when cooled to absolute zero. One has to apply at least about 25.4 or 34.4 bar (for  $T \rightarrow 0 \text{ K}$ ), respectively, to get these two isotopes in their solid state. Consequently, the helium isotopes have no triple point where gas, liquid and solid

**Table 2.3.** Properties of liquid helium

	${}^3\text{He}$	${}^4\text{He}$
Boiling point, $T_b$ (K)	3.19	4.21
Critical temperature, $T_c$ (K)	3.32	5.20
Maximum superfluid transition temperature, $T_c$ (K)	0.0025	2.1768
Density <sup>a</sup> , $\rho$ ( $\text{g cm}^{-3}$ )	0.082	0.1451
Classical molar volume <sup>a</sup> , $V_m$ ( $\text{cm}^3 \text{ mol}^{-1}$ )	12	12
Actual molar volume <sup>a</sup> , $V_m$ ( $\text{cm}^3 \text{ mol}^{-1}$ )	36.84	27.58
Melting pressure <sup>b</sup> , $P_m$ (bar)	34.39	25.36
Minimum melting pressure, $P_m$ (bar)	29.31	25.32
Gas-to-liquid volume ratio <sup>c</sup>	662	866

<sup>a</sup>At saturated vapour pressure and  $T = 0 \text{ K}$ .

<sup>b</sup>At  $T = 0 \text{ K}$ .

<sup>c</sup>Liquid at 1 K, NTP gas (300 K, 1 bar).



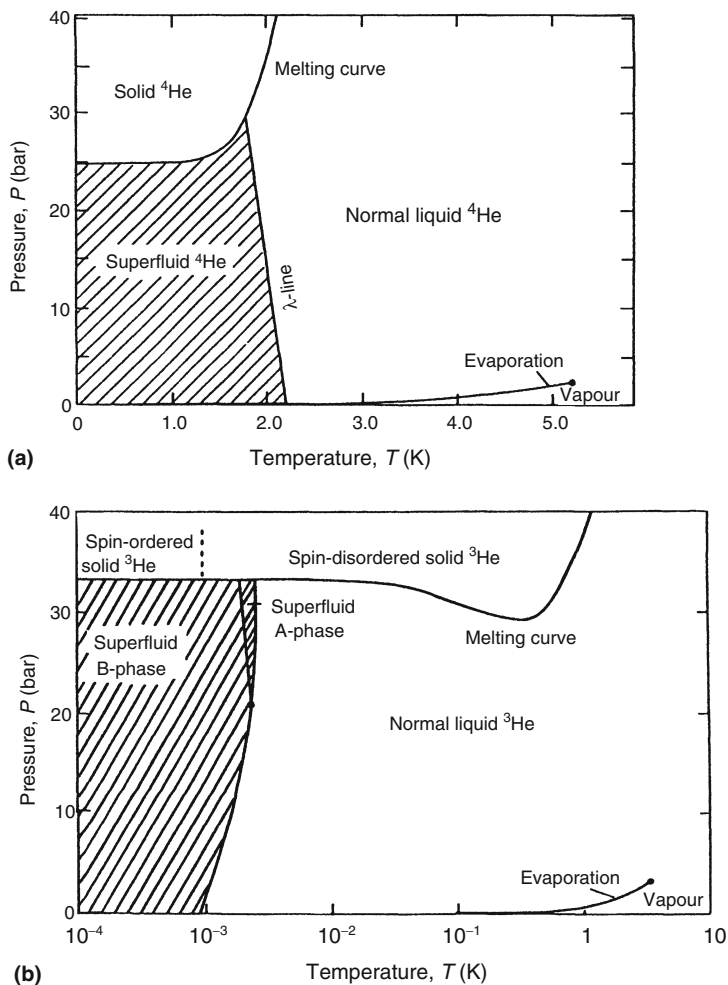


**Fig. 2.4.** Phase diagrams of (a)  ${}^4\text{He}$  and (b)  ${}^3\text{He}$ . Note the different temperature scales

phases coexist. The melting pressure of  ${}^4\text{He}$  is constant to within about  $10^{-4}$  below 1 K but for  ${}^3\text{He}$  it shows a pronounced minimum at 0.32 K (Chap. 8). Then the two liquids have a rather small density or large molar volume. The molar volume  $V_m$  of  ${}^4\text{He}$  ( ${}^3\text{He}$ ) is more than a factor of two (three) larger than one would calculate for a corresponding classical liquid.

The origin for all these observations are two essential properties of helium. First, the binding forces between the atoms are very weak. They are van der Waals forces and are weak because of the closed electronic s-shell of helium, giving rise to the absence of static dipole moments and to the smallest known atomic polarizability  $\alpha = 0.1232 \text{ cm}^3 \text{ mol}^{-1}$  (the resulting dielectric constants

for the two helium isotopes are  $\epsilon_4 = 1.0572$  and  $\epsilon_3 = 1.0426$ ). For example, these binding forces are more than an order of magnitude smaller than for hydrogen molecules with their larger polarizability, which leads to a much higher boiling temperature of  $\text{H}_2$ . Because the electronic structure of the two helium isotopes is identical, they have identical van der Waals forces and behave identically chemically. Second, due to the small atomic mass  $m$ , the two helium isotopes have a large quantum mechanical zero-point energy  $E_0$ , given by

$$E_0 = \frac{h^2}{8ma^2}, \quad (2.7)$$

where  $a = (V_m/N_0)^{1/3}$  is the radius of the sphere to which the atoms are confined, and  $N_0$  is Avogadro's number,  $6.022 \times 10^{23}$  atoms  $\text{mol}^{-1}$ .

The large zero-point energy (which is larger than the latent heat of evaporation of liquid helium, see (Table 2.1)) gives rise to a zero-point vibration amplitude which is about 1/3 of the mean separation of the atoms in the liquid state. Figure 2.5 illustrates the influence of the zero-point energy on the total energy as a function of distance between the atoms, and demonstrates why helium – in contrast to all other substances – will remain in the liquid state under its own vapour pressure even when cooled to absolute zero. Of course, due to its smaller mass the influence of the zero-point energy is more pronounced for  $^3\text{He}$ , giving rise to its lower boiling point, smaller density, smaller latent heat of evaporation and larger vapour pressure (Sect. 2.3.2).

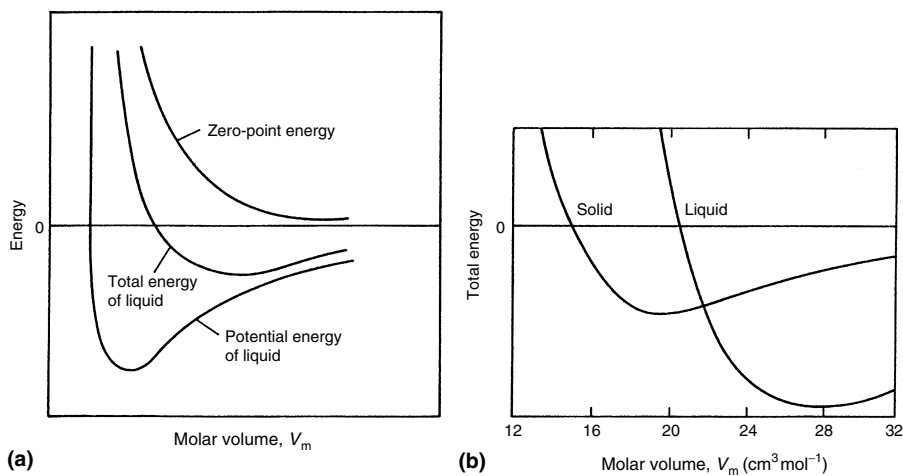


**Fig. 2.5.** (a) Zero-point and potential energies of liquid  $^4\text{He}$  as a function of molar volume. The total energy is the sum of these two energies. (b) Illustration of why the liquid state is the stable one for helium at saturated vapour pressure even at  $T = 0 \text{ K}$

Because of the strong influence of quantum effects on their properties, the helium liquids are called quantum liquids. In general, this term is used for any liquid whose kinetic (or zero-point) energy is larger than its potential (or binding) energy. To distinguish these liquids from classical liquids one introduces a quantum parameter  $\lambda = E_{\text{kin}}/E_{\text{pot}}$ . These parameters  $\lambda$  for some cryoliquids are:

liquid:	Xe	Kr	Ar	N <sub>2</sub>	Ne	H <sub>2</sub>	<sup>4</sup> He	<sup>3</sup> He
$\lambda$ :	0.06	0.10	0.19	0.23	0.59	1.73	2.64	3.05

indicating that hydrogen and the helium isotopes are quantum liquids in this sense.

### 2.3.2 Latent Heat of Evaporation and Vapour Pressure

The latent heat of evaporation  $L$  and the vapour pressure  $P_{\text{vap}}$  are important properties that determine whether a liquid is suitable for use as a refrigerant. For the helium isotopes both these properties are dramatically different from the values of the corresponding classical liquids due to the large zero-point energy. For example, for <sup>4</sup>He the latent heat of evaporation is only about one-third of its value for the corresponding classical liquid. Due to the small heat of evaporation of helium (Fig. 2.6), liquid helium baths have a rather

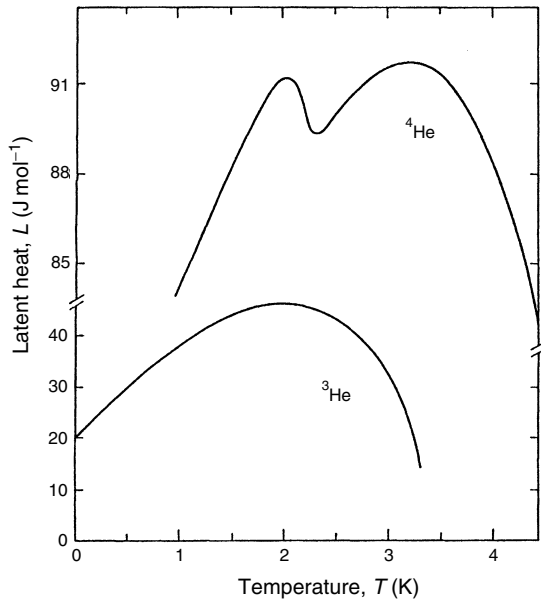


**Fig. 2.6.** Latent heats of evaporation of <sup>3</sup>He and <sup>4</sup>He. Note the change of vertical scale

small cooling power (it is very easy to evaporate them). Therefore, all low-temperature experiments require efficient shielding against introduction of heat from the surroundings, e.g., heat due to radiation, heat along supports to the experiments, or heat due to the measurements one wants to perform at low temperatures. This will be discussed later when we discuss the design of low-temperature equipment. The dip in  $L$  for  $^4\text{He}$  at 2.2K is due to the superfluid transition occurring at this temperature, which will be discussed in Sect. 2.3.3.

The vapour pressure can be calculated, at least to a first approximation, from the Clausius–Clapeyron equation

$$\left[\frac{dP}{dT}\right]_{\text{vap}} = \frac{S_{\text{gas}} - S_{\text{liq}}}{V_{\text{m, gas}} - V_{\text{m, liq}}}, \quad (2.8)$$

where  $S$  is the entropy and  $V_{\text{m}}$  the molar volume.

If we take into account that the difference in the entropies of the liquid and gaseous phases is  $L/T$ , that the molar volume of the liquid is much smaller than the molar volume of the gas, and that in a rough approximation the molar volume of helium gas is given by the ideal gas equation  $V_{\text{gas}} \cong RT/P$ , then we obtain

$$\left[\frac{dP}{dT}\right]_{\text{vap}} \cong \frac{L(T)P}{RT^2}, \quad (2.9)$$

and eventually arrive at our result for the vapour pressure

$$P_{\text{vap}} \propto e^{-L/RT}, \quad (2.10)$$

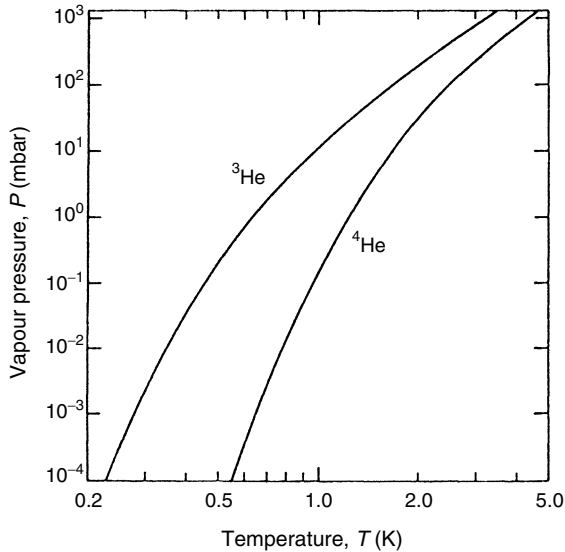


**Fig. 2.7.** Vapour pressures of liquid  $^3\text{He}$  and liquid  $^4\text{He}$

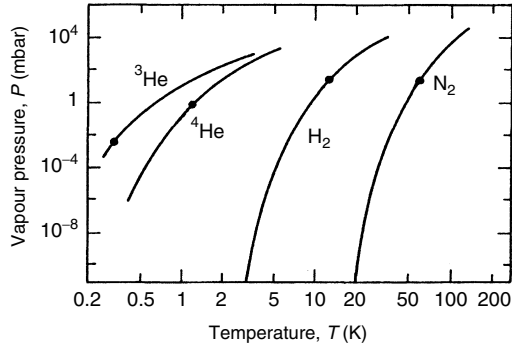


**Fig. 2.8.** Vapour pressures of various cryoliquids. The dots indicate the practical lower limits for the temperatures which can be obtained by reducing the vapour pressure above these liquids

if we make the further approximation that  $L \cong \text{const.}$  (Fig. 2.6). Therefore, the vapour pressure decreases roughly exponentially with decreasing temperature, as shown in Fig. 2.7 for the helium isotopes and in Fig. 2.8 for several cryoliquids (for more details on vapour pressures see Sects. 11.2 and 12.2).

One can take advantage of this pronounced temperature dependence of the vapour pressure in several ways. In the Kelvin temperature range, the vapour pressures of all substances except helium are extremely low (Fig. 2.8). Therefore, the surfaces in a low-temperature apparatus cooled to Kelvin temperatures, e.g., by liquid helium, are extremely efficient “pumps”. If one has pumped on the vacuum space of a low-temperature apparatus at high temperatures, the valve to the pumping system should be closed when the apparatus has reached the Kelvin temperature range by introducing liquid helium because the cold surfaces can improve the vacuum by several orders of magnitude by condensing the remaining gas molecules. Usually it is much better to do this than to keep the valve to the pumping system open, because after a while the cold surfaces may pump molecules from the pumping system (such as crack products of the pump oil) into the cryostat. This “cryopumping” is utilized commercially in so-called cryopumps available from various suppliers.

Second, one can pump on the vapour above a liquid, for example above a liquid-helium bath, to obtain temperatures below the normal (1 bar) boiling point. If one pumps away atoms from the vapour phase, the most energetic (“hottest”) atoms will leave the liquid to replenish the vapour. Therefore the mean energy of the liquid will decrease; it will cool. For a pumped-on liquid bath where  $\dot{n}$  particles/time are moved to the vapour phase, the cooling power is given by

$$\dot{Q} = \dot{n}(H_{\text{liq}} - H_{\text{vap}}) = \dot{n}\dot{L}. \quad (2.11)$$

Usually a pump with a constant-volume pumping speed  $\dot{V}$  is used and therefore the mass flow  $\dot{n}$  across the liquid–vapour boundary is proportional to the vapour pressure

$$\dot{n} \propto P_{\text{vap}}(T), \quad (2.12)$$

giving a cooling power

$$\dot{Q} \propto LP_{\text{vap}} \propto e^{-1/T}. \quad (2.13)$$

This last equation demonstrates that the cooling power decreases rapidly with decreasing temperature because the vapour pressure decreases rapidly with decreasing temperature and pumping becomes less and less efficient. Eventually there is almost no vapour left, resulting in a limit for the minimum temperature obtainable by pumping on a bath of an evaporating cryoliquid. This limit is reached when the refrigeration due to evaporation of atoms is balanced by the external heat flowing to the bath. The practical low-temperature limits determined by experimental parameters are typically about 1.3 K for  $^4\text{He}$  and 0.3 K for  $^3\text{He}$  (Fig. 2.8).

The temperature dependence of the vapour pressure of liquid helium is well known and can be used for vapour-pressure thermometry (Sect. 12.2). By measuring the vapour pressure above a liquid-helium bath (or other liquids at higher temperatures) one can read the temperature from the corresponding vapour pressure table. In fact, the helium-vapour pressure scale represents the low-temperature part of the international temperature scale ITS-90 (Sect. 11.2).

### 2.3.3 Specific Heat

Many of the basic properties of a material, including liquid helium, are revealed by its specific heat. First of all, the specific heat of liquid helium is very large compared to the specific heat of other materials at low temperatures (Fig. 2.9). For example, at about 1.5 K the specific heat of 1 g of  $^3\text{He}$  or  $^4\text{He}$  is of the order of  $1 \text{ J K}^{-1}$  whereas the specific heat of 1 g of Cu is only about  $10^{-5} \text{ J K}^{-1}$  at this temperature. This remarkable fact is of great cryotechnical importance for low-temperature physics. It means that the thermal behavior, for example the thermal response time, of a low-temperature apparatus is in most cases determined by the amount and thermal behavior of the liquid helium it contains. In addition, the latent heat of evaporation of liquid helium – even though it is rather small compared to the latent heat of other materials – is large compared to the specific heat of other materials at low temperatures, enabling us to cool other materials, e.g., a metal, by liquid helium. Both properties mean that the temperature of an experiment rapidly follows any temperature change of its refrigerating helium bath.

At low temperatures the properties of materials are strongly influenced by statistical or quantum effects. This is particularly important for the specific heat of the helium isotopes. As Fig. 2.10 demonstrates, the specific heat of  $^4\text{He}$  has a pronounced maximum at about 2.17 K, indicating a phase transition to a new state of this liquid. The detection of this phase transition came as a great surprise to scientists. It was not expected that anything interesting could happen at low temperatures with this rather simple liquid composed of

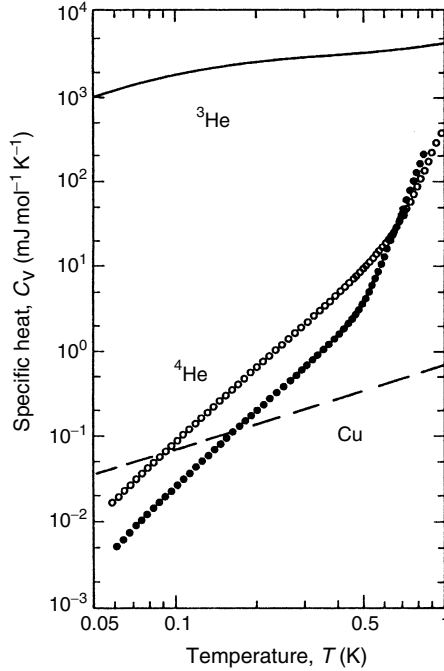


**Fig. 2.9.** Specific heat of liquid  $^4\text{He}$  at vapour pressure ( $27.58\text{ cm}^3\text{ mol}^{-1}$ ,  $\circ$ ) and at about 22 bar ( $23.55\text{ cm}^3\text{ mol}^{-1}$ ,  $\bullet$ ) [2.25] compared to the specific heats of liquid  $^3\text{He}$  at vapour pressure [2.26] and of Cu

inert spherical atoms. Therefore, when L.J. Dana and H. Kamerlingh Onnes measured the specific heat of liquid helium in the 1920s and saw an “anomalous” increase of the specific heat at about 2 K, they did not publish the data points at those temperatures, believing that they resulted from some experimental artefacts. Later W.H. Keesom and K. Clusius (1932) in the same laboratory of the University of Leiden measured the specific heat of liquid helium again and again saw the pronounced peak of the specific heat. They did believe in their data and realized that a phase transition occurred in this liquid at that temperature, the transition to the unique superfluid state of  $^4\text{He}$ . W.H. Keesom introduced the names He I for the normal liquid above the transition temperature and He II for the superfluid liquid below it. The history of the specific heat of liquid  $^4\text{He}$  is one of the important examples in physics that one should never disregard any apparently “anomalous” data or data points unless one has good reason not to trust one’s own measurements. The specific heat maximum of liquid  $^4\text{He}$  near 2.2 K has been measured with increasing temperature resolution over the past decades (Fig. 2.10). Today it is known with a sub-nanokelvin temperature resolution, and these very precise measurements are one of the most important testing grounds for modern

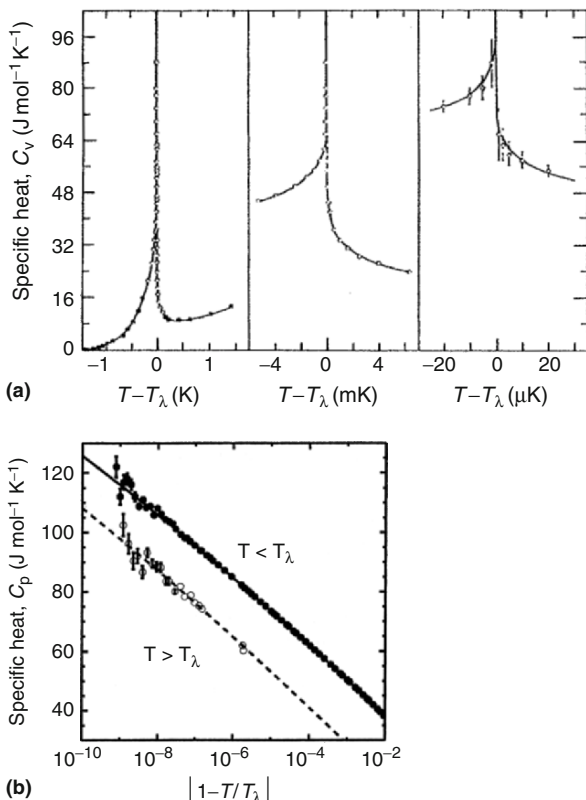


**Fig. 2.10.** Specific heat of liquid  $^4\text{He}$  at temperatures close to its superfluid transition. (a) With increasing  $T$ -resolution on a linear temperature scale [2.27] and (b) on a logarithmic temperature scale. Reprinted with permission from [2.30]; copyright (2003) Am. Phys. Soc.. These latter data have been taken in flight on earth orbit to avoid the rounding of the phase transition by gravitationally caused pressure gradients in the liquid sample of finite height. For the applied high-resolution thermometry see Sect. 12.9

theories of phase transitions [2.27–2.30]. It is a demonstration of the model character of the superfluid transition of liquid helium for phase transitions and the very advanced state of low-temperature thermometry (Chaps. 11 and 12, in particular Sect. 12.9). Helium is an extremely good system for the study of properties with a very high temperature resolution near a critical temperature due to its extreme purity (all other materials are “frozen-out”). Therefore the sharpness of the transition. The characteristic shape of the specific heat maximum has led to the term  $\lambda$ -transition for the superfluid transition of  $^4\text{He}$  occurring at the  $\lambda$ -temperature  $T_\lambda = 2.1768 \text{ K}$  at saturated vapour pressure. The  $\lambda$ -temperature decreases with increasing pressure to a value of  $1.7673 \text{ K}$  at the melting line (Fig. 2.4).



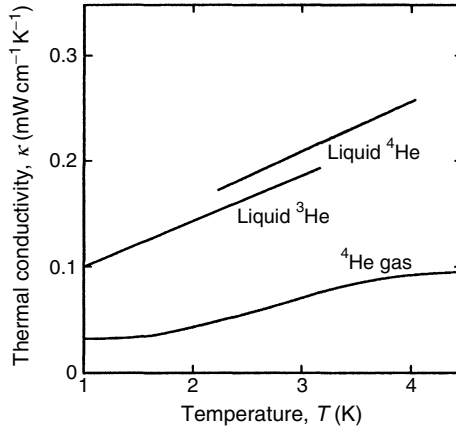


**Fig. 2.11.** Thermal conductivities of gaseous and liquid helium [2.31]

Above the  $\lambda$ -transition,  ${}^4\text{He}$  behaves essentially like a classical fluid or in some respects – because of its low density – almost like a classical gas (Fig. 2.11). But below  $T_\lambda$  due to its (Bose–Einstein like) condensation in momentum space, its entropy and specific heat decrease rapidly with temperature (Fig. 2.9). Between 1 and about 2 K the specific heat of  ${}^4\text{He}$  has a strong temperature dependence due to so-called roton excitations. Finally, below 0.6 K, the specific heat decreases with  $T^3$  due to phonon-like excitations, as for an insulating Debye solid (Sect. 3.1.1) [2.17–2.24].

The isotope  ${}^3\text{He}$  has a nuclear spin  $I = 1/2$ . It is therefore a Fermi particle and has to obey Fermi statistics and the Pauli principle. This liquid has many properties in common with the “conducting Fermi liquid” composed of electrons in metals, which are also spin-1/2 particles. For example, the specific heat of  ${}^3\text{He}$  obeys  $C \propto T$  at low enough temperatures. This result and some other properties of  ${}^3\text{He}$  will be discussed in Sect. 2.3.6 and in Chaps. 7 and 8.

### 2.3.4 Transport Properties of Liquid ${}^4\text{He}$ : Thermal Conductivity and Viscosity

In its normal fluid state above  $T = 2.2$  K, liquid  ${}^4\text{He}$ , due to its low density, shows transport properties almost like a classical gas (Fig. 2.11). The same applies to liquid  ${}^3\text{He}$  at temperatures above 0.1 K. Due to its low thermal conductivity *above* 2.2 K [it is about a factor of 10 ( $10^4$ ) lower than the thermal conductivity of stainless steel (Cu), see Sect. 3.3] liquid  ${}^4\text{He}$  I boils with strong bubbling. When one pumps on liquid  ${}^4\text{He}$  I (or liquid  ${}^3\text{He}$ ), bubbles of vapour form within the liquid and the liquid is agitated when they rise to the surface. The bubbles form because the bulk of the liquid is hotter than its pumped surface. In an experiment employing liquid helium it is very likely that there are large thermal gradients in the liquid at these temperatures.

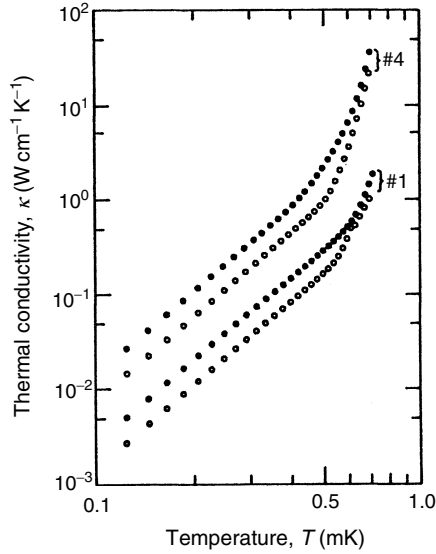


**Fig. 2.12.** Thermal conductivity of liquid  ${}^4\text{He}$  at 2 bar (●) and 20 bar (○) in tubes of 1.38 mm (#1) and 7.97 mm (#4) diameter [2.32]

This is of importance, for example, when the vapour pressure of liquid helium is used for thermometry (Sect.12.2). Conversely, *below* 2.2 K, in the superfluid state, under ideal experimental conditions (heat flow  $Q \rightarrow 0$ ) the thermal conductivity of  ${}^4\text{He}$  II is infinite; for realistic conditions it is finite but quite large (Fig. 2.12). The very high thermal conductivity of superfluid helium makes this material a very efficient medium for establishing temperature homogeneity or for transporting heat. For example, at these temperatures the liquid does not boil as other liquids do if heated from the bottom or if they are pumped, because for boiling by creation of bubbles and their transport to the surface it is necessary that a temperature gradient is established. This is impossible in liquid helium below  $T_\lambda$  if the heat current is not so large that it “destroys” the superfluid state. In the superfluid state helium atoms evaporate exclusively from the surface and the liquid is “quiet” because no more bubbles are formed. The thermal conductivity of superfluid  ${}^4\text{He}$  below 0.4 K, in the phonon regime, and at  $P \leq 2$  bar is given by

$$\kappa_4 \propto 20dT^3(\text{W}(\text{K cm})^{-1}), \quad (2.14)$$

where  $d$  is the diameter of the  ${}^4\text{He}$  column in centimeters (Fig. 2.12) [2.32]. As a result, the thermal conductivity of superfluid  ${}^4\text{He}$  is quite high under most experimental conditions, comparable to that of a metal. For the physics of heat transport in superfluid  ${}^4\text{He}$ , the reader should consult the literature specializing on this quantum liquid [2.17–2.24].

Because the thermal conductivity of superfluid helium can be very large (or ideally infinitely large), temperature waves or entropy waves can propagate in this unusual liquid. This wave propagation is called second sound to distinguish it from the usual first sound, the density waves. The velocity of second sound in  ${}^4\text{He II}$  is about an order of magnitude smaller than the velocity of first sound at  $1\text{ K} \leq T \leq 2\text{ K}$  [2.17–2.24].

In the superfluid state, liquid helium has a vanishing viscosity,  $\eta_s = 0$ , for flow through fine capillaries or holes; it is indeed “superfluid” if the flow velocity does not exceed a critical value (corresponding to a critical current in metallic superconductors). The vanishing viscosity allows superfluid helium to flow in a persistent mode as the persistent supercurrents in a metallic superconductor do. Apparatus which seems to be leak-tight for  $T \geq T_\lambda$  may show a leak at lower temperatures if it comes into contact with superfluid helium because this liquid can flow through minute cracks or holes which are impermeable to viscous materials. This is a very efficient way of detecting extremely small leaks. On the other hand, it is, of course, a nuisance because apparatus which seems to be leak-tight at higher temperatures may suddenly develop a so-called superleak when in contact with superfluid helium.

The transport properties of liquid  ${}^3\text{He}$  will be briefly discussed in Sect. 2.3.6.

### 2.3.5 Superfluid Film Flow

The walls of a container which is partly filled with liquid helium are coated with a film of helium via the adsorption of atoms from the vapour phase. Due to the rather strong van der Waals interaction which a substrate exerts on helium atoms, the first layer of  ${}^4\text{He}$  on a substrate is solid and the liquid film above it is relatively thick, typically 30 nm at SVP (see below). Usually, due to its viscosity, such a film is immobile. However, in the superfluid state with

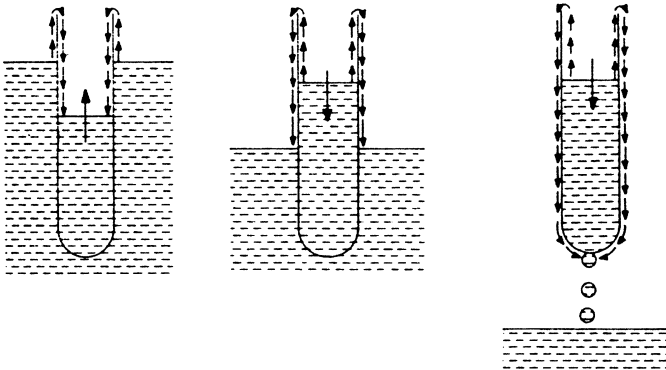


**Fig. 2.13.** Due to its superfluid properties  ${}^4\text{He II}$  can leave a container via superfluid film flow over the walls

$\eta_s = 0$ , the film can move. If two containers which are partly filled with liquid He II to different levels are connected, their levels will equalize by means of frictionless flow of the He II film from one container to the other one driven by the difference in gravitational potential (Fig. 2.13); the film acts as though being siphoned. This superfluid film flow [2.17, 2.33] will lead to an enhanced evaporation rate from  $^4\text{He}$  baths at  $T < T_\lambda$  because the superfluid film flows to hotter places and evaporates there.

Here, I will calculate the thickness  $d$  of a helium film at a height  $h$  above the bulk liquid level (Fig. 2.14). For the chemical potential of the film we have

$$\mu_{\text{film}} = \mu_0 + mgh - \alpha/d^n, \quad (2.15)$$

where  $\mu_0$  is the chemical potential of the bulk liquid, and  $mgh$  is the gravitational term. The last term in the above equation is the van der Waals potential which the substrate supplies to the film (with  $n = 3$  for  $d \leq 5$  nm;  $n = 4$  for  $d \geq 10$  nm). For thin films, the van der Waals constant is  $\alpha/k_B = (10\text{--}200 \text{ (K)}) \times (\text{no. of helium layers})^3$  for various solid substrates [2.33]. In thermal equilibrium an atom has to have the same chemical potential on the surface of the bulk liquid and on the surface of the film ( $\mu_{\text{film}} = \mu_0$ ); this condition leads to (for  $d \leq 5$  nm)

$$d = (\alpha/mgh)^{1/3}. \quad (2.16)$$

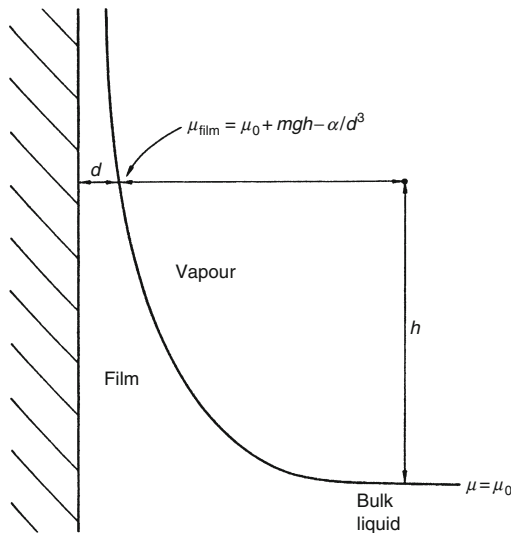


**Fig. 2.14.** Profile of a helium film on a vertical wall in equilibrium with its bulk liquid and with its saturated vapour. The chemical potential is given for the bulk liquid ( $\mu_0$ ) and for the liquid film ( $\mu_{\text{film}}$ ) at a height  $h$  above the bulk liquid

A typical value is

$$d \simeq 30 \text{ h}^{-1/3} \quad (2.17)$$

with  $h$  in cm and  $d$  in nm; but, of course,  $d$  strongly depends on the cleanliness and structure of the surface of the substrate.

If there is gas but no bulk liquid present we have an “unsaturated film” whose thickness depends on the gas pressure  $P$ . The gas pressure at height  $h$  is

$$P(h) = P_{\text{sat}} e^{-mgh/k_B T}. \quad (2.18)$$

Correspondingly, in (2.15),  $mgh$  has to be replaced by  $k_B T / \ln(P_{\text{sat}}/P)$ , and we obtain for the film thickness

$$d = \left[ \frac{\alpha}{k_B T \ln(P_{\text{sat}}/P)} \right]^{1/3}, \quad (2.19)$$

showing that the film thickness decreases by lowering the vapor pressure.

For a typical critical superfluid velocity of a  $^4\text{He}$  film,  $v_{\text{s,crit}} \approx 30 \text{ cm s}^{-1}$ , we determine the volume flow rate out of a beaker of radius  $R = 5 \text{ mm}$

$$\dot{V}_{\text{liq}} = 2R\pi d v_{\text{s,crit}} \approx 1 \text{ cm}^3 \text{ h}^{-1} \quad \text{or} \quad \dot{V}_{\text{gas}} \approx 11 \text{ h}^{-1}. \quad (2.20)$$

We then find for a pump with a volume pumping rate  $\dot{V}_{\text{pump}} = 10^4 \text{ h}^{-1}$  at  $P = 1 \text{ bar}$  that the minimum pressure to which this pump can pump such a helium bath from which a superfluid film is creeping is

$$P_{\text{min}} = P \dot{V}_{\text{gas}} / \dot{V}_{\text{pump}} \approx 10^{-3} \text{ bar} \quad (10^{-4} \text{ bar if } R = 50 \text{ mm}). \quad (2.21)$$

Correspondingly, the minimum helium-bath temperature will be about 1 K, showing that one has to consider the film flow rate quite carefully and possibly has to reduce it, for example by a constriction of about 1 mm diameter in the pumping tube (Chap. 7). In addition, one has to remember that dirt on a surface can offer a very large effective surface area for the film flow.

### 2.3.6 Liquid $^3\text{He}$ and $^3\text{He}$ – $^4\text{He}$ Mixtures at Millikelvin Temperatures

Because  $^3\text{He}$  atoms are Fermi particles, single  $^3\text{He}$  atoms cannot undergo the analogue of a Bose momentum condensation into a superfluid state as the bosons  $^4\text{He}$  do at  $T_\lambda$ . However, there exists a weak attractive interaction between  $^3\text{He}$  atoms in the liquid which gives rise to pairing of two  $^3\text{He}$  atoms. Like the paired conduction electrons in a superconducting metal, the paired  $^3\text{He}$  atoms then behave like bosons and can undergo a transition into a superfluid state. Because the pairing forces are rather weak, this transition occurs only at 2.4 (0.92) mK for  $P = P_{\text{melting}}(P_{\text{svp}})$  (see Fig. 2.4 and Table 11.5). The exciting properties of superfluid  $^3\text{He}$  have been the driving force for the development of refrigeration techniques to  $T < 3 \text{ mK}$  and they have been the object of intense investigations since the detection of superfluid  $^3\text{He}$  in 1972

[2.34,2.35]. They are discussed in several relevant publications [2.19–2.24,2.36–2.43]. As for  $^4\text{He}$ , where the experiments on the superfluid properties in the late 1920s and 1930s were restricted to the few laboratories which had access to the low Kelvin temperature range, particularly Leiden, the experiments on the superfluid properties of  $^3\text{He}$  in the 1970s were restricted to the few laboratories which then had access to the low-millikelvin-temperature range, particularly Cornell, San Diego and Helsinki. Because we are interested in this book in the cryotechnological aspects of materials, I will not discuss superfluid  $^3\text{He}$  but just remind you of those properties of liquid  $^3\text{He}$  above its superfluid transition that are of importance in cryotechnical applications of this Fermi liquid.

Liquid  $^3\text{He}$ , due to its smaller mass, has a larger zero-point energy than liquid  $^4\text{He}$ . It therefore has an even lower density and in the almost “classical” regime, for  $T > 0.1\text{ K}$ , behaves even more like a dense classical gas. For example, its specific heat is almost  $T$ -independent, as it should be according to the Dulong–Petit law (Sect. 3.1.1), at  $T \approx 0.5\text{ K}$  (Fig. 2.16). Liquid  $^3\text{He}$  is a spin-1/2 particle; it is a fermion with an anti-symmetric wave function. At lower temperatures, its properties then become in many respects increasingly similar to The well-known Fermi liquid composed of the conduction electrons in metals, obeying Fermi statistics, too. The properties of liquid  $^3\text{He}$  at low temperatures are therefore fundamentally different from those of  $^4\text{He}$ . From about  $0.1\text{ K}$  down to the superfluid transition temperature they can be accounted for by Landau’s Fermi liquid theory [2.17,2.19–2.24,2.36,2.39–2.45]. This theory describes the liquid as a system of free fermions with its properties rescaled by the interatomic interactions. Due to the Pauli principle the  $^3\text{He}$  atoms have to fill energy states up to the Fermi energy  $E_F$  (Fig. 3.3). Because  $E_F/k_B \approx 1\text{ K}$  for  $^3\text{He}$  but  $E_F/k_B \approx 10^4\text{ K}$  for electrons, and because the specific heat  $C \propto T/T_F$  for a Fermi liquid (Sect. 3.1.2, Fig. 2.15), the specific heat of  $^3\text{He}$  at low temperatures is very large compared to the specific heat of metals (Fig. 2.9). This linear  $T$ -dependence of  $C$  is obeyed by  $^3\text{He}$  only up to about ten millikelvin (Fig. 2.15, Sect. 7.1). At higher temperatures, the specific heat of  $^3\text{He}$  shows a plateau and then increases again with increasing temperature (Fig. 2.16). In the low millikelvin temperature range when  $^3\text{He}$  enters its superfluid state, the specific heat, of course, deviates from a linear temperature dependence.

The transport properties of liquid  $^3\text{He}$  in the Fermi-liquid temperature range, too, show a distinct  $T$ -dependence. For example, the thermal conductivity  $\kappa_3$  increases as  $T^{-1}$  at  $T \ll T_F$  (Figs. 2.17 and 2.18), and its viscosity  $\eta_3$  increases as  $T^{-2}$  in the low millikelvin temperature range (Fig. 2.19), making  $^3\text{He}$  a very viscous but well-conducting fluid at low temperatures above its superfluid transition. These temperature dependences can easily be understood. The mean free path  $\lambda$  of  $^3\text{He}$  particles in the liquid is limited by scattering with other  $^3\text{He}$  particles. A two-body collision for Fermi particles is proportional to  $(T/T_F)^2$ , because the number of particles and the number of empty states into which they can scatter near to the Fermi energy are both proportional to temperature. Hence, we have  $\lambda \propto T^{-2}$ , and with  $C \propto T$  and

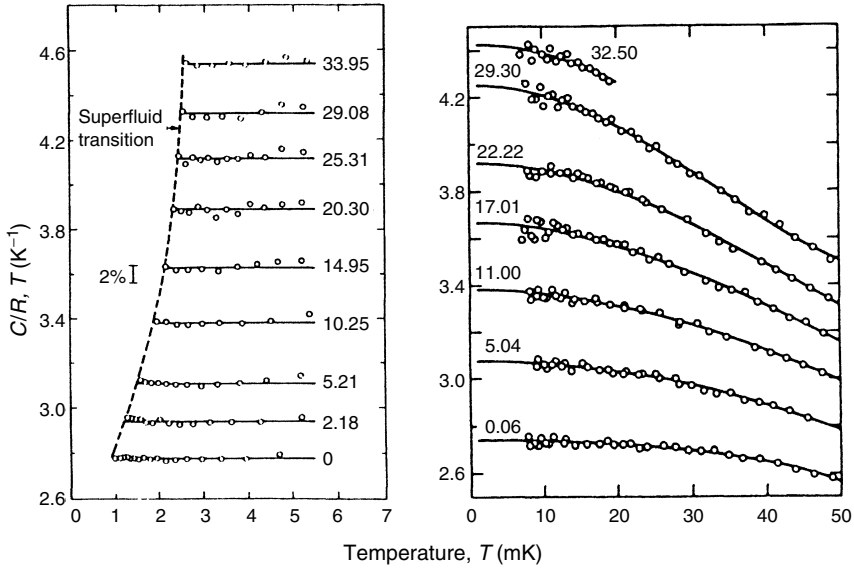


**Fig. 2.15.** Specific heat  $C$  divided by the gas constant  $R$  times temperature  $T$  of liquid  $^3\text{He}$  at millikelvin temperatures at the given pressures (in bar). Note the different scales [2.26]

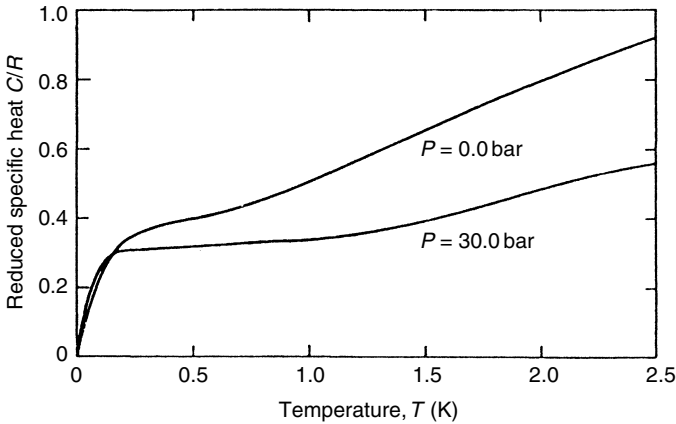


**Fig. 2.16.** Specific heat  $C$  (divided by the gas constant  $R$ ) of liquid  $^3\text{He}$  at two given pressures (after data from [2.26])

$v_F = \text{const.}$  we find from (3.30) that  $\kappa_3 \propto T^{-1}$  (and  $\eta_3 \propto T^{-2}$ ) for  $T \ll T_F$ . At higher temperatures  $\kappa_3$  and  $\eta_3$  show a more complicated behavior.

It is important to remember that the thermal conductivity of this Fermi liquid becomes equal to the thermal conductivity of metallic conductors at

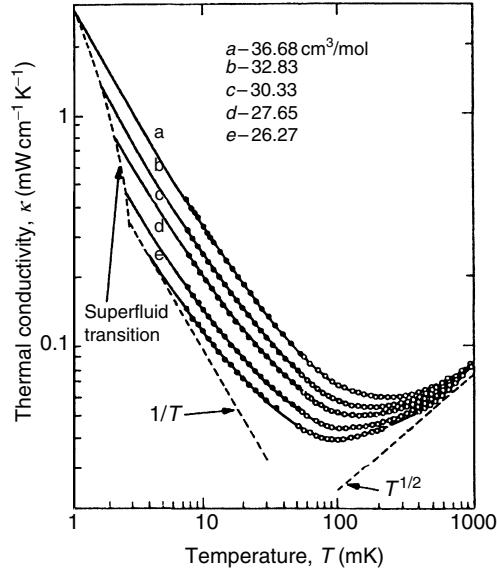


**Fig. 2.17.** Thermal conductivity of liquid  ${}^3\text{He}$  at the given molar volumes [2.48]. At low temperatures, one finds the Fermi-liquid behavior  $k \propto T^{-1}$

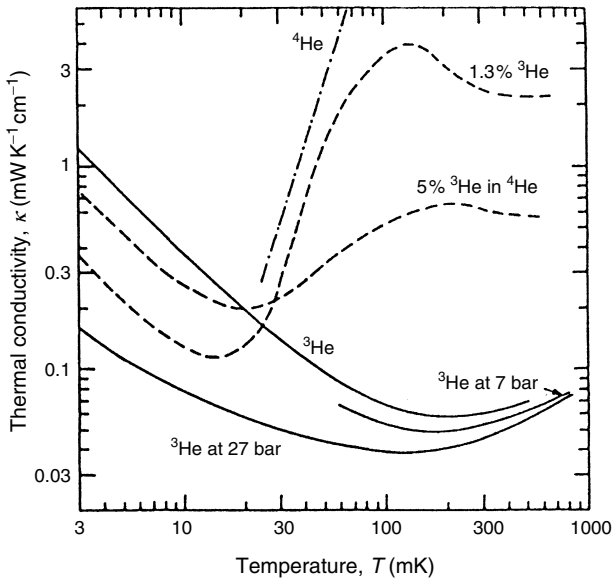


**Fig. 2.18.** Thermal conductivities of liquid  ${}^3\text{He}$ , liquid  ${}^4\text{He}$ , and dilute  ${}^3\text{He}$ - ${}^4\text{He}$  mixtures; unless otherwise indicated, the data are taken at SVP [2.50]. (This reference should also be consulted for references to the original literature). More-recent data for the thermal conductivities of  ${}^4\text{He}$  and  ${}^3\text{He}$  are given in Figs. 2.12 and 2.17



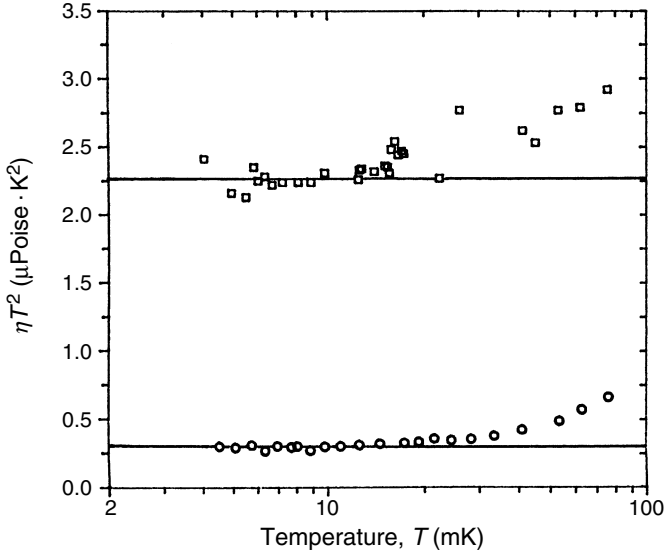


**Fig. 2.19.** Viscosity  $\eta$  of liquid  ${}^3\text{He}$  ( $\square$ ) and of a 6.8%  ${}^3\text{He}$ - ${}^4\text{He}$  He mixture ( $\circ$ ) at 0.4 bar multiplied by  $T^2$  as a function of temperature. The solid lines represent the Fermi liquid behavior  $\eta \propto T^2$  [2.52]

about 2 mK! In addition, the viscosity of liquid  ${}^3\text{He}$  increases to that of light machine oil just above its superfluid transition temperature!

In liquid  ${}^3\text{He}$ - ${}^4\text{He}$  mixtures at low temperatures [2.17, 2.23, 2.24, 2.46, 2.49, 2.51], say at  $T < 0.1\text{ K}$ , the superfluid  ${}^4\text{He}$  component contains very few excitations (phonons and rotons); it acts essentially as an inert background influencing mostly the effective mass of the interacting  ${}^3\text{He}$  Fermi particles. Hence, the helium mixtures behave as Fermi liquids, more dilute than pure liquid  ${}^3\text{He}$  but with the same Fermi-liquid temperature dependences of their properties but altered absolute values. In particular,  $C/T$  (Fig. 7.5),  $\kappa T$  (Fig. 2.18), and  $\eta T^2$  (Fig. 2.19) are temperature independent at low enough temperatures,  $T \ll T_{\text{Fermi}}$ , as for pure liquid  ${}^3\text{He}$ . The advantage of the helium mixtures is the possibility to change their concentration and hence  $T_{\text{Fermi}}$  and to study the resulting changes of properties for testing theoretical predictions.

This short discussion of the properties of liquid helium relevant for its application in low-temperature experiments, in particular as a refrigerant, should be sufficient for our purpose. For a general discussion of the properties of liquid, in particular, superfluid helium, whose properties can be phenomenologically understood in terms of a “two-fluid model”, the reader should consult the special literature on this subject given in the list of references for this chapter. Some of the properties of liquid  ${}^3\text{He}$  will be discussed again in connection with Pomeranchuk cooling in Chap. 8, and liquid mixtures of the two helium isotopes will be considered in more detail in Chap. 7 when we discuss the dilution refrigerator.

## Problems

**2.1.** Calculate the energy difference between one mole of normal  $\text{H}_2$  at room temperature and one mole of *para*- $\text{H}_2$ .

**2.2.** Determine the nuclear spin  $I$  and rotator quantum number  $J$  for *ortho*- and *para*-deuterium. What is the *para*-deuterium concentration at room temperature and at 20 K?

**2.3.** Why does the mixed molecule HD not show an *ortho*-*para* or *para*-*ortho* conversion?

**2.4.** Deduce (2.7) by considering a free particle in a spherical cavity. Compare the result for liquid  $^4\text{He}$  with its latent heat of evaporation.

**2.5.** Calculate the de Boer parameter  $\lambda = E_{\text{kin}}/E_{\text{pot}}$  (see Table 2.3) for  $\text{H}_2$  assuming for  $E_{\text{kin}}$  the zero-point energy and for  $E_{\text{pot}}$  the Lennard-Jones potential

$$U(R) = \epsilon[(\sigma/R)^{12} - (\sigma/R)^6] \quad \text{with } \epsilon = 5 \times 10^{-15} \text{ erg and } \sigma = 2.96 \text{ \AA}.$$

**2.6.** Calculate the binding energy of a helium atom at the surface of liquid helium at 1 K (latent heat  $L = 2.2 \text{ kJ/l}$ ).

**2.7.** Calculate the Debye temperature (3.7) corresponding to the heat capacity of liquid  $^4\text{He}$  for  $T < 60$ ; 0.5 K (Fig. 2.9).

**2.8.** Calculate the thickness of an unsaturated  $^4\text{He}$  film on a horizontal glass substrate ( $\alpha = k_B 30 \text{ K layers}^3$ ) at  $P/P_{\text{sat}} = 0.5$ .

**2.9.** To which pressure does one have to pump  $^4\text{He}$  in a tube of 1 cm diameter and 20 cm length so that the heat transported by the remaining superfluid film is less than  $10^{-4} \text{ W}$  if the ends of the tube are at 2 and 1 K, see (2.19, 2.20) and Fig. 2.12?